

Characterisation of low background CaWO_4 crystals for CRESST-III

Angelina Kinast^{1*}, G. Angloher², S. Banik^{3,4}, G. Benato⁵, A. Bento^{2,6}, A. Bertolini², R. Breier⁷, C. Bucci⁵, J. Burkhart³, L. Canonica², A. D'Addabbo⁵, S. Di Lorenzo⁵, L. Einfalt^{3,4}, A. Erb^{1,8}, F. v. Feilitzsch¹, N. Ferreira Iachellini², S. Fichtinger³, D. Fuchs², A. Fuss^{3,4}, A. Garai², V. M. Ghete³, S. Gerster⁹, P. Gorla⁵, P. V. Guillaumon⁵, S. Gupta³, D. Hauff², M. Jeřkovský⁷, J. Jochum⁹, M. Kaznacheeva¹, H. Kluck³, H. Kraus¹⁰, A. Langenkämper^{1,2}, M. Mancuso², L. Marini^{5,11}, L. Meyer⁹, Valentyna Mokina³, A. Nilima², M. Olmi⁵, T. Ortmann¹, C. Pagliarone^{5,12}, L. Pattavina^{1,5}, F. Petricca², W. Potzel¹, P. Povinec⁷, F. Pröbst², F. Pucci², F. Reindl^{3,4}, J. Rothe¹, K. Schäffner², J. Schieck^{3,4}, D. Schmiedmayer^{3,4}, S. Schönert¹, C. Schwertner^{3,4}, M. Stahlberg², L. Stodolsky², C. Strandhagen⁹, R. Strauss¹, I. Usherov⁹, F. Wagner³, M. Willers¹ and V. Zema²

* angelina.kinast@tum.de



14th International Conference on Identification of Dark Matter
Vienna, Austria, 18-22 July 2022
doi:[10.21468/SciPostPhysProc.12](https://doi.org/10.21468/SciPostPhysProc.12)

Abstract

The CRESST-III experiment aims at the direct detection of dark matter particles via their elastic scattering off nuclei in a scintillating CaWO_4 target crystal. For many years CaWO_4 crystals have successfully been produced in-house at Technische Universität München with a focus on high radiopurity. To further improve the CaWO_4 crystals, an extensive chemical purification of the raw materials has been performed and the crystal TUM93 was produced from this powder. We present results from an α -decay rate analysis performed on 344 days of data collected in the ongoing CRESST-III data-taking campaign. The α -decay rate could significantly be reduced.



Copyright A. Kinast *et al.*

This work is licensed under the Creative Commons

[Attribution 4.0 International License](https://creativecommons.org/licenses/by/4.0/).

Published by the SciPost Foundation.

Received 03-10-2022

Accepted 02-05-2023

Published 04-07-2023

doi:[10.21468/SciPostPhysProc.12.031](https://doi.org/10.21468/SciPostPhysProc.12.031)



Check for updates

1 Physik-Department, Technische Universität München, D-85747 Garching, Germany

2 Max-Planck-Institut für Physik, D-80805 München, Germany

3 Institut für Hochenergiephysik der Österreichischen Akademie der Wissenschaften,
A-1050 Wien, Austria

4 Atominstitut, Technische Universität Wien, A-1020 Wien, Austria

5 INFN, Laboratori Nazionali del Gran Sasso, I-67100 Assergi, Italy

6 LIBPhys-UC, Departamento de Física, Universidade de Coimbra,
P3004 516 Coimbra, Portugal

7 Comenius University, Faculty of Mathematics, Physics and Informatics,
84248 Bratislava, Slovakia

8 Walther-Meißner-Institut für Tieftemperaturforschung, D-85748 Garching, Germany

9 Eberhard-Karls-Universität Tübingen, D-72076 Tübingen, Germany

10 Department of Physics, University of Oxford, Oxford OX1 3RH, United Kingdom

11 GSSI-Gran Sasso Science Institute, I-67100 L'Aquila, Italy

12 Dipartimento di Ingegneria Civile e Meccanica, Università degli Studi di Cassino
e del Lazio Meridionale, I-03043 Cassino, Italy

1 Introduction

CRESST-III (Cryogenic Rare Event Search with Superconducting Thermometers) [1] aims at the direct detection of dark matter (DM) using cryogenic calorimeters. The standard CRESST-III module consists of a scintillating 24 g CaWO_4 single crystal as a target. It is operated at ≈ 10 mK temperature and is equipped with a transition edge sensor (TES) read out by a SQUID (Superconducting QUantum Interference Device) for a precise measurement of the energy deposited by a particle interaction within the crystal. In addition to the CaWO_4 crystal, a light detector (also equipped with a TES) is read out in coincidence. This enables discrimination between electromagnetic interactions (background-like events), α -decays (background events, less relative scintillation light) and nuclear recoils (signal-like events, least relative scintillation light) due to the different relative fraction of scintillation light produced. CRESST-III detectors reach thresholds as low as 30.1 eV, allowing a very sensitive measurement of particle recoil energies [1].

One key point for the excellent performance of these detectors is the quality of the target crystals, including a high radiopurity of the CaWO_4 material, to minimise backgrounds resulting from natural decay chains. Especially β -decays can cause events in the region of interest for DM searches. To assure a high quality of the CaWO_4 crystals, they have been produced in-house at Technische Universität München (TUM) for many years [2]. In this way, every step of the production is controlled and optimised. The crystal TUM40 operated in CRESST-II showed an excellent performance and a lower background compared to commercially purchased crystals operated in the same CRESST run [3].

To further improve the radiopurity, an extensive chemical purification of the raw materials and the CaWO_4 powder has been developed at TUM. HPGe screening of the powder shows promising results for an improved radiopurity, however, the sensitivity of this method is limited and only limits on the radiopurity could be stated [4]. From this purified powder, the crystal TUM93 has been produced in 2019. In total three CRESST-III target crystals were cut from the ingot and mounted into CRESST-III modules named TUM93A, TUM93B and TUM93C. The crystal TUM93A was cut from the top of the ingot and is, due to segregation effects during crystal growth, expected to be the most radiopure crystal among the three detector crystals [5]. All modules are currently being operated in the ongoing CRESST-III data-taking campaign started in November 2020. A radiopurity analysis focusing on α -decays detected in ≈ 344 days of this data-taking campaign is presented in this work. For this analysis, a new approach for energy reconstruction has been developed and is presented in the following.

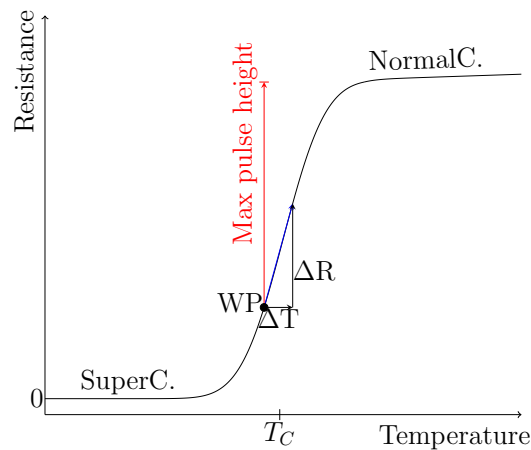


Figure 1: Working principle of a TES. The TES is heated into its transition in the so-called working point (WP). A particle interaction results in a temperature increase ΔT which in turn results in a resistance increase ΔR . The maximum resistance increase is defined by the resistance difference between the normal conducting resistance and the WP resistance.

2 Analysis

The output of both the phonon detector (PD) and the light detector (LD) are recorded with a continuous data acquisition to enable a dead-time free stream of data which is further processed offline. In this way, the analysis can be adapted to the specific need of e.g. the low-energy DM analysis or, as in this case, the analysis of α -decays with energies of several MeV. Still, the reconstruction of such highly energetic events with CRESST-III detectors and standard analysis approaches is not possible, due to the optimisation of the detectors to lowest energies.

One reason for this is the working principle of the TES used for the signal readout of both the PD and the LD. A TES is a thin W-film operated at a temperature between the superconducting and normal conducting phase (see Figure 1). Energy deposition in the crystal heats the TES (ΔT) and results in a resistance change (ΔR) proportional to the energy deposition. To maximise this resistance change, and lower the detector threshold, a steep transition is required. When the energy deposited in the crystal heats the TES completely into its normal conducting phase (like for α -decays), a maximum resistance change and in turn a maximum pulse height is observed which stays constant until the TES cools back into its transition region. In addition, such high energy depositions cause a fast rise in the resistance which cannot be followed by the SQUID electronics, which is losing magnetic flux quanta and changes the absolute baseline voltage of the stream. Figure 2 (left) shows an example of an α -event recorded in the detector TUM93A. The pulse is flat at the top as the TES is in its fully normal conducting state and the baseline level is lower at the end of the pulse compared to the baseline level before the pulse due to the flux quantum loss (FQL). These pulses cannot be reconstructed with standard pulse reconstruction methods as they cannot handle the FQLs. Hence, the new reconstruction method was developed which uses the length of the flat part of the pulse (its saturation time), which is determined by the time the pulse needs to reach 90% of its maximum voltage. The saturation time is indicated by the blue line and is used to reconstruct the energy deposited in the crystal, as it gives a measure of how long the TES needs to come back to its operating temperature. Together with a correction for the SQUID FQLs in which the difference between

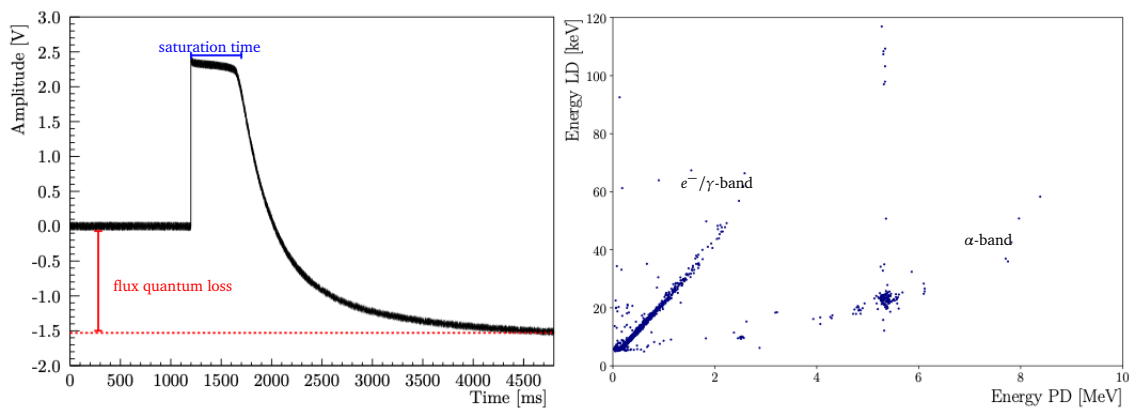


Figure 2: Left: Typical event recorded by the PD for an α -decay in the CaWO_4 crystal. The pulse has a changing baseline level due to flux quantum losses in the SQUID. In addition, the pulse is flat at the top as the TES is completely normal conducting in this time period. Right: Calibrated scatter plot for the data set of TUM93A. For both, the LD and the PD, the reconstruction was performed using the saturation time. Two bands are visible, the e^-/γ -band on the left and the α -band on the right.

the baseline level before and after the pulse is determined, the energy of α -decay pulses can be reconstructed in both the PD and the LD.

In the next step some data selection criteria are applied to the data: Coincidences with the muon veto and the artificial heat pulses sent to the detector for stabilisation and monitoring are excluded. In addition, electronic artefacts like SQUID-resets are removed from the data set and events with too slow a change in resistance are excluded from the data set to prevent the wrong reconstruction of too low energetic pulses. No additional data selection criteria are applied to avoid the possibility of removing α -decay events from the data. The resulting scatter plot of the reconstructed energy in the LD against the reconstructed energy in the PD is shown in Figure 2 (right). The e^-/γ -band, also reconstructed with the saturation time method, is visible as the steep band on the left, as the relative light output is higher for electromagnetic interactions. The α -decay band is nicely separated from the electromagnetic background. The α -spectrum is calibrated using four lines present in the data selected from a wide energy range. As a cross-check the end of the e^-/γ -band at 2.6 MeV is used. The ^{180}W decay line at 2.52 MeV, ^{226}Ra at 4.88 MeV, the ^{210}Po surface background line at 5.30 MeV and the ^{218}Po line at 6.11 MeV are fitted by an exponential function as the saturation time has an exponential dependence on the deposited energy. The pulse model on which this assumption is based is published in [6]. The measurement time is corrected for dead times caused by muon veto coincidences and the artificial heat pulses sent to the detector for its stabilisation.

3 Results

The calibrated α -spectra for the detectors TUM93A (6.53 kg·d exposure), TUM93B (6.89 kg·d exposure) and TUM93C (6.87 kg·d exposure) are shown in Figure 3. Prominent features are the ^{180}W decay at 2.52 MeV and the two ^{210}Po lines at 5.41 MeV (full energy detected by the crystal) and at 5.30 MeV for decays where the daughter nucleus escapes from the surface of the crystal and does not deposit energy in it. The strong presence of both peaks compared to other energy areas of the spectra hints towards surface contamination of the CaWO_4 crystals with ^{222}Rn and with ^{210}Pb , which decayed to ^{210}Po . A background model is currently being developed for a more detailed study of the spectra of all three crystals.

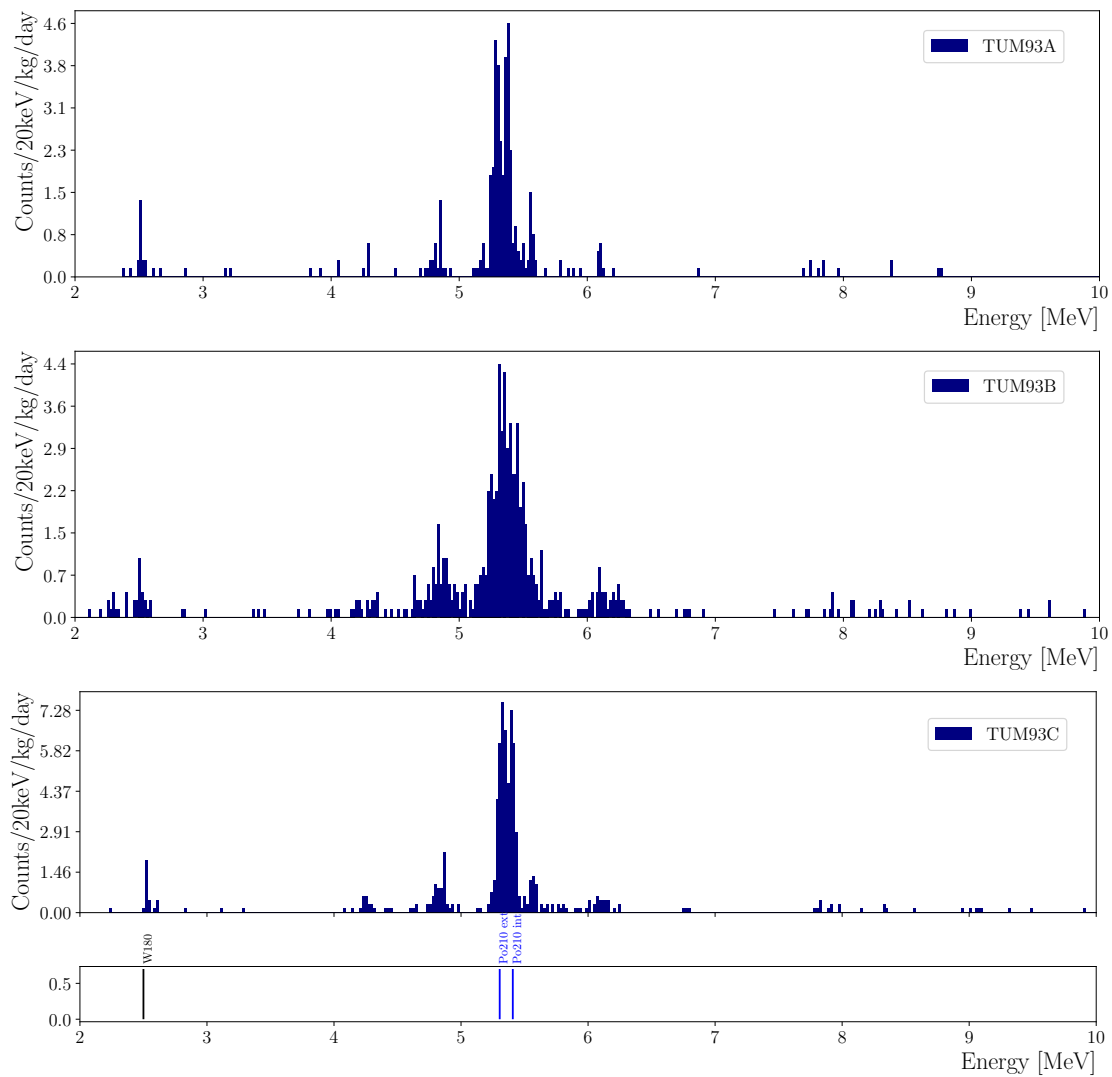


Figure 3: Final α -spectra for all TUM93 detectors. All detectors feature two prominent lines at 5.30 MeV and 5.41 MeV. Both result from the decay of ^{210}Po which hints toward surface contamination with ^{222}Rn . At 2.52 MeV the α -decay of ^{180}W is visible.

Even though the spectra seem to be dominated by surface contamination, a conservative α -decay rate from natural decay chains in the TUM93 crystals was calculated by summing up all events in the energy region from 3 MeV up to 10 MeV, shown in Table 1.

The rate difference in the three crystals, even though they were cut from the same ingot, has two origins. First, during crystal growth impurities are less likely to be built into the crystal lattice compared to the crystal atoms. Hence, the impurity concentration in the melt increases and in turn also along the growth axis in the crystal. This process is called segregation. In addition, the high presence of the 5.30 MeV ^{210}Po line indicates a comparably high surface contamination which can be different for each detector crystal. The highest observed rate in TUM93B could also hint toward a mix-up of the crystals TUM93B and TUM93C during detector mounting.

Comparing these conservative limits to the α -activity of e.g. the crystal TUM40, which was studied in detail in [3, 7] with an α -decay rate from natural decay chains of $3.080 \frac{\text{mBq}}{\text{kg}}$ this yields a minimum impurity reduction factor of >5.97 for TUM93A, >3.18 for TUM93B

Table 1: Conservative α -decay rate of isotopes of the three natural decay chains (^{238}U , ^{235}U , ^{232}Th) in an energy range of 3 MeV to 10 MeV. All events are assumed to be of intrinsic origin even though there are hints that the two main contributions are from surface contamination with ^{210}Po .

Detector	α -Activity $\left[\frac{\mu\text{Bq}}{\text{kg}}\right]$
TUM93A	516 ± 62
TUM93B	919 ± 79
TUM93C	761 ± 76

and >3.85 for TUM93C. These results show a significant impact of the chemical purification on the α -decay rate in TUM93. The e^-/γ -band activity and the activity of single α -decaying isotopes are currently being studied with the help of simulations.

Acknowledgements

Funding information This work has been funded by the Deutsche Forschungsgemeinschaft (DFG, German Research Foundation) under Germany's Excellence Strategy - EXC 2094 - 390783311 and through the Sonderforschungsbereich (Collaborative Research Center) SFB1258 'Neutrinos and Dark Matter in Astro- and Particle Physics', by the BMBF 05A20WO1 and 05A20VTA and by the Austrian science fund (FWF): I5420-N, W1252-N27. FW was supported through the Austrian research promotion agency (FFG), project ML4CPD. SG was supported through the FWF project STRONG-DM (FG1). The Bratislava group acknowledges a partial support provided by the Slovak Research and Development Agency (project APVV-15-0576).

References

- [1] A. H. Abdelhameed et al., *First results from the CRESST-III low-mass dark matter program*, Phys. Rev. D **100**, 102002 (2019), doi:[10.1103/PhysRevD.100.102002](https://doi.org/10.1103/PhysRevD.100.102002).
- [2] A. Erb and J.-C. Lanfranchi, *Growth of high-purity scintillating CaWO_4 single crystals for the low-temperature direct dark matter search experiments CRESST-II and EURECA*, CrystEngComm **15**, 2301 (2013), doi:[10.1039/C2CE26554K](https://doi.org/10.1039/C2CE26554K).
- [3] R. Strauss et al., *Beta/gamma and alpha backgrounds in CRESST-II phase 2*, J. Cosmol. Astropart. Phys. **2015**, 030 (2015), doi:[10.1088/1475-7516/2015/06/030](https://doi.org/10.1088/1475-7516/2015/06/030).
- [4] A. Münster, *High-purity CaWO_4 single crystals for direct dark matter search with the CRESST experiment*, Ph.D. thesis, Technische Universität München (2017).
- [5] A. Kinast et al., *Improving the quality of CaWO_4 target crystals for CRESST*, J. Low Temp. Phys. **209**, 1128 (2022), doi:[10.1007/s10909-022-02743-7](https://doi.org/10.1007/s10909-022-02743-7).
- [6] F. Pröbst et al., *Model for cryogenic particle detectors with superconducting phase transition thermometers*, J. Low Temp. Phys. **100**, 69 (1995), doi:[10.1007/BF00753837](https://doi.org/10.1007/BF00753837).

- [7] A. H. Abdelhameed et al., *Erratum to: Geant4-based electromagnetic background model for the CRESST dark matter experiment*, Eur. Phys. J. C **79**, 987 (2019), doi:[10.1140/epjc/s10052-019-7504-y](https://doi.org/10.1140/epjc/s10052-019-7504-y).